ELSEVIER

Biochimica et Biophysica Acta 1330 (1997) 284–292

BIOCHIMICA ET BIOPHYSICA ACTA
BBA

Lateral diffusion and conductance properties of a fluorescein-labelled alamethicin in planar lipid bilayers

O. Helluin [a], J.-Y. Dugast [a], G. Molle [a], A.R. Mackie [b], S. Ladha [b], H. Duclohier [a,*]

[a] *UMR 6522 CNRS-Université de Rouen (IFRMP 23), 76821 Mont Saint Aignan France*
[b] *Institute of Food Research, Norwich Research Park, Colney, Norwich NR4 7UA, UK*

Received 27 May 1997; revised 5 June 1997; accepted 5 June 1997

Abstract

In order to follow alamethicin diffusion within membranes under conditions of pore-formation, a fluorescein isothiocyanate (FITC) analogue was synthesized. To test the influence of the fluorescent probe addition on the pore-forming activity of the new analogue, macroscopic and single-channel experiments into planar lipid bilayers were performed. Although the apparent mean number of monomers per conducting aggregate was equivalent, the voltage-dependence of the new analogue was slightly reduced and hysteresses were broader, in agreement with the much longer duration of the open single-channels. Thus, the conducting aggregates seem to be stabilized by the introduction of the probe, presumably through the interaction of the conjugated cycles with the lipid headgroups, while the added steric hindrance may account for the slightly higher conductances of the open substates. Lateral diffusion of the labelled peptide associated with the bilayer was then investigated by the fluorescence recovery after photobleaching technique. Under applied voltage, associated with high conductance, D, the lateral diffusion coefficient, was reduced by 50% when compared to peptide at rest. These results provide new independent experimental evidence for a voltage-driven insertion of the highly mobile surface-associated peptide into the bilayer as a prominent step in pore formation. © 1997 Elsevier Science B.V.

Keywords: Alamethicin; Fluorescent analogue; Conductance; Planar lipid bilayer; Lateral diffusion

1. Introduction

Alamethicin is still the best-studied membrane-active peptide and its value as a model for voltage-gated ion conduction is underlined in a number of studies (for reviews, see [1–4]). Isolated from the fungus *Trichoderma viride*, this amphipathic peptide promotes strongly voltage-dependent conductances in planar lipid bilayers and, under some conditions, excitability phenomena [5]. Despite alamethicin being rich in Aibs (α-aminoisobutyric acid or U in the single-letter code), these non-coded residues as well as Pro14 were nevertheless shown to be non-essential for the conduction properties [6,7]. Although alamethicin's voltage-dependent gating still remains a matter of debate [models accounting for voltage-dependent structural changes, phase partitioning or insertion have been proposed (for review, see e.g. [4])], there seems to be a consensus for the barrel–stave model [8,9] to account for the high voltage- and concentration-dependencies of macroscopic conductance and for the multi-levels seen in single-channel recordings.

* Corresponding author. Fax: (+33) 235146704; E-mail: Herve.Duclohier@univ-rouen.fr

PII S0005-2736(97)00139-9

In this model, which now serves as a paradigm for the general architecture of the central conducting part of many ion channels or their peptide models [10–12], the pore is made up by the juxtaposition of the hydrophilic sectors of neighbouring helices forming a transmembrane bundle [13]. The uptake and release of alamethicin monomers by this bundle is the simplest explanation accounting for the non-integral conductance increments. There is general agreement between conductance values and a geometric model for a pore of varying size, depending upon the number of monomers or helical rods [1,14,15].

In this scheme, it is obvious that the lateral diffusion of monomers within the lipid bilayer is a step of paramount importance and it would be desirable to dispose of direct measurements in this respect [16]. Likewise, it may be assumed that the conducting aggregates of different sizes would experience different diffusion regimes. To this end, we have recently developed a fluorescence recovery after photobleaching (FRAP) apparatus that has been adapted for lateral diffusion in planar lipid bilayers and which is also amenable to electrical measurements [17]. This new experimental system was tested with conventional membrane fluidity modifiers (cholesterol, calcium with negatively charged bilayers...) using fluorescently labelled phospholipids. Interestingly, it was also found that alamethicin did slightly reduce the lipid lateral mobility. As a second step, it was necessary to dispose of a fluorescently labelled analogue of alamethicin whose essential conductance properties could be preserved. Due to its high emission quantum yield in aqueous solution and an absorption wavelength matching the output of argon lasers (at 488 nm), fluorescein isothiocyanate (FITC) is certainly one of the most versatile low molecular weight and long wavelength fluorophores.

In this paper, we thus describe the strategy adopted for the synthesis of a fluorescein–alamethicin, its chromatographic purification, together with its mass spectrum and fragmentation to check the identity of the final product. To test the influence of the rather bulky added group on the pore-forming activity of this new analogue, macroscopic and single-channel conductance experiments into planar lipid bilayers were performed. It will be shown that the main functional characteristics of the initial alamethicin are preserved, i.e. the labelled analogue still functions according to the barrel–stave model, and that the different conducting aggregates are greatly stabilized. Finally, the FRAP method was implemented to illustrate the feasibility of direct investigations of lateral diffusion of a pore-former within planar lipid bilayers under applied voltage.

2. Materials and methods

2.1. Materials

Alamethicin (Alm) was obtained from Sigma. This is a 70:30 mixture of Ala_6 and Aib_6 [determined by high-performance liquid chromatography (HPLC) and fast atom bombardment mass spectroscopy (FAB–MS)] in the Gln_{18} version or "Rf 50", which was our starting material here. t-Boc glycine and FITC (Product number F-143) were purchased from Bachem (Switzerland) and Molecular Probes (Eugene, OR, USA), respectively. Palmitoyloleoylphosphocholine (POPC) and dioleoylphosphocholine (DOPE) were obtained from Avanti Polar Lipids (Alabaster, AL, USA). FAB–MS was performed on a ZAB HF model from VG Analytical at the "Service Central d'Analyses du CNRS" (Solaize, France) with 10–20 μg samples dissolved in thioglycerol.

2.2. Synthesis, purification and mass characterization of Alm–Gly–FITC

The general strategy of coupling isothiocyanate to amine groups in proteins and peptides has been extensively discussed, e.g. in [18]. Specifically, we adapted two protocols described earlier [19,20], but with an intervening achiral residue (Gly) coupled to the C-terminal amino-alcohol and both providing flexibility and the primary amine required for isothiocyanate coupling. In a first step, the anhydride of t-Boc–Gly was synthesized: t-Boc–Gly (875 mg) and *N,N'*-dicyclohexylcarbodiimide (515 mg) were dissolved in 2.5 ml of CH_2Cl_2 and 7.5 ml of dry *N,N'*-dimethylformamide (DMF). After stirring at room temperature during 30 min, this mixture was filtered to discard dicyclohexylurea and the anhydride filtrate was saved as "solution 1".

A 15-mg amount of alamethicin was then dissolved in 1.5 ml of a solution containing 20 mg of

dimethylaminopyridine (DMAP) in 1.6 ml of dry DMF and then 1.5 ml of solution 1 was added. This mixture was stirred overnight. The solvent was then removed in vacuo and the residue was resuspended in 10 ml of methanol before being applied to a Sephadex LH 20 column (35 × 1 cm) running in methanol. Alm–Gly–t-Boc was eluted in the first peak. Final purification was performed by reversed-phase HPLC on a preparative C_{18} column under a 50% acetonitrile (AcCN)–H_2O isocratic solution. Two main peaks were observed and analyzed by FAB–MS. The first peak, $(M + Na)^+ = 2143.7$, was the expected peptide (7 mg yield), while the second peak was identified as des-Ala–Aib Alm–Gly–t-Boc, $(M + Na)^+ = 2157.4$, where Ala_6 was replaced by Aib_6.

The above 7 mg of Alm–Gly–t-Boc were treated in 700 μl of CH_2Cl_2 and 300 μl of trifluoroacetic acid (TFA) for 30 min. After removing the solvent in vacuo, the solid was redissolved in 2 ml of a 1:1 solution of DMF–50 mM phosphate, pH 7. Then, 40 mg of FITC were added to this mixture and the reaction was allowed to proceed for 3 h at room temperature. The final product was purified on a preparative C_{18} column using an AcCN–H_2O gradient and the peaks were detected at 226 and 488 nm. The final yield after lyophilization was 3.7 mg (i.e. an overall yield of ~ 25%).

2.3. Fluorescence controls and conductance assays in planar lipid bilayers

Fluorescence excitation and emission spectra of liquid samples in quartz cuvettes of 1 cm optical pathlength were recorded with an Hitachi Model F-2000 spectrofluorimeter. Functional assays in planar lipid bilayers were carried out with methods already described, e.g. [6]. Briefly, in macroscopic and single-channel conductance experiments, virtually solvent-free bilayers were formed by the apposition of two lipid monolayers [21] on a 100–150 μm hole in a 10 μm thick PTFE film sandwiched between two glass half cells and pretreated with hexane–hexadecane (40:1, v/v). The lipid mixture used was 1,2-POPC–DOPE (7:3) dissolved (0.5%, w/w) in hexane. Bilayer formation was monitored by the capacitance response and, before adding the peptide, the bare membrane was tested under an applied voltage in order to control the absence of channel-like events. The voltage and current sign conventions are the usual ones and the electrolyte solution was 1 M KCl, 5 mM HEPES buffered, pH 7.4. Single-channel events were digitally stored and subsequently analyzed (Satori v. 3.01 software from Intracel, Royston, UK).

2.4. Fluorescence recovery after photobleaching measurements of the lateral diffusion of the labelled peptide in planar lipid bilayers under applied voltage

The planar lipid bilayers (PLBs) were prepared as previously described [17]. Briefly, a 25-mm thick PTFE septum (Goodfellow, Cambridge, UK) with a hole of 200–300 μm diameter in the centre was clamped into a specially designed chamber that allowed simultaneous electrical (conductance and capacitance) and FRAP measurements to be made. Prior to membrane formation, the hole in the septum was coated on each side with 1 μl of 1% (v/v) hexadecane in hexane. The hexane was allowed to evaporate. To form Montal and Mueller [21] planar lipid bilayers, buffer (1 M KCl, 5 mM HEPES, pH 7.4) was added to each side of the chamber such that the level was above the hole in the septum. Lipid (1,2-POPC–DOPE, 7:3, m/m) containing 1 mol.% labelled peptide was spread from a hexane solution on the buffer surface in the *trans*-side of the chamber. On the *cis*-side of the chamber, lipid (1,2-POPC–DOPE, 7:3, m/m) without labelled peptide was spread. The hexane was allowed to evaporate. The buffer level on the *trans*-side was lowered below the hole in the PTFE septum and then raised back to its original level. PLB formation was monitored optically through a microscope, and electrically via capacitance measurements.

FRAP was used to measure the lateral diffusion coefficient of the labelled peptide associated with the PLBs. After formation of the planar lipid bilayer, a laser beam (488 nm) was focused on the centre of the bilayer. The laser beam was of Gaussian cross-sectional intensity, with half-width at $1/e^2$ height of the laser beam at its point of focus equal to 3.3 μm (spot radius). All experiments were performed at a controlled room temperature of 23°C. Ten FRAP curves were collected for every measurement and were averaged before analysis and derivation of D, the lateral diffusion coefficient, as described earlier [17].

3. Results and discussion

To keep perturbations brought by the added probe to a minimum, we avoided interfering with the transmembrane parts. Thus, the C-terminus part is the most suitable part for coupling the fluorescent group to. The fixation of FITC requires a primary amine but the C-terminus part is an alcohol (phenylanalinol). To overcome this difficulty, we esterified the terminal phenylalanilol using the anhydride of N-Boc glycine (a non-chiral amino-acid). After N-deprotection, Alm–Gly was obtained in almost quantitative yield and then the FITC group was condensed on the free NH_2 of glycine. After HPLC purification, Alm–Gly–FITC was characterized by mass spectroscopy ($M + H^+ = 2410.3$) and adequate fragmentation (not shown), due to the presence of the acylium fragment Alm–Gly (2021.4) after the loss of FITC group, and the usual fragment (the first thirteen residues on the N-terminus, $M + H^+ = 1189.6$) left after breaking at Pro14.

3.1. Fluorescence controls

To assert the integrity of the fluorescence reporter after its coupling to the alamethicin main chain via the additional glycine residue, we compared excitation and emission spectra of the labelled alamethicin with those of FITC alone, under similar conditions. Apart from a small blue-shift (−3 nm) of both spectra for FITC–Gly–Alam, which can be tentatively assigned to the influence (hydrophobic) of alamethicin, Fig. 1 shows that the photophysical properties of a $5 \cdot 10^{-5}$ M methanolic solution of labelled alamethicin (the stock solution used in macroscopic conductance experiments, see below) are quite similar to those of FITC alone (same concentration in methanol). Comparable peaks point to a one-to-one ratio for probe/alamethicin, in agreement with the mass spectrum and fragmentation of the purified and labelled product.

3.2. Macroscopic conductance

In order to test the ion channel behaviour of this new analogue, macroscopic and single-channel experiments were carried out and conductance properties were compared with those of the parent molecule.

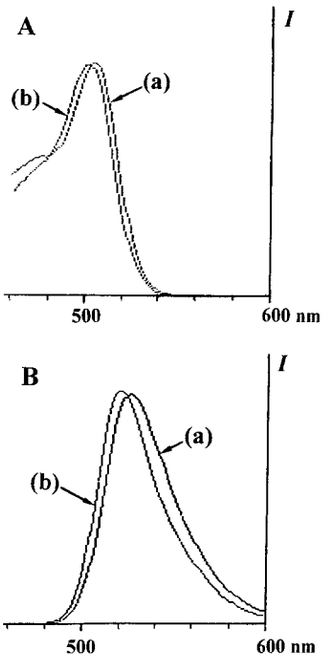

Fig. 1. Fluorescence excitation (A) and emission (B) spectra of FITC alone (a) and FITC-labelled alamethicin (b), both in methanol solution at $5 \cdot 10^{-5}$ M. Excitation and emission wavelengths are 505 and 526 nm for FITC alone, and $\lambda_{ex} = 502$ nm and $\lambda_{em} = 522$ nm in the case of FITC–Gly–Alam. *Y*-axes: Fluorescence intensities in arbitrary units.

Macroscopic current–voltage (I–V) curves are useful to screen the functional properties of new potential channel-formers and allow comparisons between analogues. In this configuration, hundreds to thousands of conducting aggregates can be expressed in large bilayers submitted to slow voltage ramps (~ 1 min per cycle) and at relatively high peptide concentrations.

Fig. 2 shows macroscopic I–V curves for the new labelled-analogue and for the Rf 50 component (or neutral form) of alamethicin, both at two concentrations differing by an order of magnitude. Compared to the responses that are typical of alamethicin behaviour [22], I–V curves recorded with FITC–alamethicin point to a reduced voltage sensitivity (as illustrated by the steepness of the exponential branches), but this was associated with increased concentration dependence (a ten-fold concentration increase results in a larger shift of the I–V curves) and even more conspicuously, much broader hystereses (between the rising and falling limbs of the

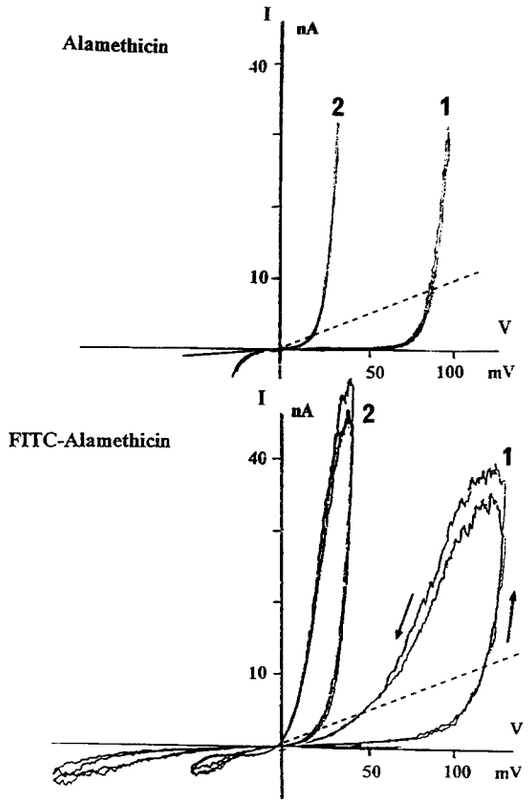

Fig. 2. Macroscopic current–voltage curves for alamethicin (Rf 50) and its fluorescein-labelled analogue. Curves 1 and 2, shown in the upper part, are for an Alm concentrations of $4 \cdot 10^{-8}$ and $4 \cdot 10^{-7}$ M, respectively, while curves 1 and 2 in the lower part are for $2.5 \cdot 10^{-8}$ and $2.5 \cdot 10^{-7}$ M FITC–Gly–Alm. In each case, two responses to the voltage-ramp were superimposed to ensure equilibrium. Dotted lines represent a reference conductance of 100 nS, which allows one to define the characteristic voltages, V_c. Arrows indicate parts of the current response corresponding to rising and falling voltage ramps.

responses). This last point reflects the longer duration for the open channels, as confirmed below in the single-channel analysis.

These I–V curves were analyzed according to the treatment previously proposed for alamethicin [23]. The pertinent parameters are: (i) V_e, the voltage increment producing an e-fold change in conductance and (ii) V_a, the voltage shifts of V_c, the characteristic or threshold voltages (for which the rising limbs cross an arbitrary reference conductance, usually about ten-fold that of the bare membrane conductance) produced by an e-fold change in peptide concentration. N_{app}, the apparent and mean number of monomers building up the conducting aggregates is then simply estimated as V_a/V_e [23]. It can be seen from Table 1 that despite the significantly different voltage- and concentration-dependencies displayed by the two analogues, their effects compensate in the ratio to yield quite similar mean numbers of monomers. Note that N_{app} for the neutral form of alamethicin (Rf 50, i.e. Gln18) is much lower than for the charged form (Rf 30, Glu18): five vs. eight–ten [24,25], reflecting either a less efficient membrane partitioning or the involvement of electrostatic repulsion in the building up of larger aggregates. With the latter analogue (Rf 30), V_a amounts to about 50–60 mV, such that with an equivalent or slightly increased voltage sensitivity, the size of Rf 30 conducting aggregates are larger (more monomers delineate the pore). Although these two natural analogues were recently reinvestigated as regards their single-channel behaviour (''persistent'' and ''non-persistent channels'', see [25]), there was, as yet, little available comparative data at the macroscopic conductance level.

3.3. Single-channel conductances

In Fig. 3, the single channel current recordings displayed by alamethicin Rf 50 and its FITC analogue are compared. Examination of these representative traces point to the same multistate behaviour, but, most conspicuously, to a drastic increase of the open lifetimes with the FITC analogue. The main single-channel conductance parameters of the two

Table 1
Comparison of macroscopic conductance data for alamethicin Rf 50 and its fluorescein-labelled analogue (FITC–Gly–alamethicin Rf 50) and taken from the current–voltage curves shown in Fig. 2

	Concentration (M)	V_c (mV)	V_a (mV)	V_e (mV)	N_{app}	$N_{rounded}$
Alamethicin Rf 50	$4 \cdot 10^{-8}$	84 ± 3	28	6	4.7	4–5
	$4 \cdot 10^{-7}$	17 ± 2				
FITC–Gly–Alam	$2.5 \cdot 10^{-8}$	117	44	10	4.4	4–5
	$2.5 \cdot 10^{-7}$	20				

Table 2
Single-channel conductances (in pS) of the substates displayed by alamethicin Rf 50 at 140 mV and by FITC–Gly–Alam at 80 mV in 1 M KCl

Substates	1	2	3	4	5	6
Alamethicin Rf 50	50	250	1100	2250	3650	5250
FITC–Gly–Alam	60	270	1310	2830	4350	6000

Temperature, 25°C.

peptides are listed in Tables 2 and 3. The addition of Gly–FITC significantly increases the single channel conductance of the substates. This could be induced by steric hindrance of the FITC group placed laterally in the conducting aggregates, off the channel mouth. Nevertheless, the normalized sequences of subconductance ratios:

1:5:22:45:73:105 for alamethicin Rf50,

and

1:4.5:22:47:73:100 for alm Rf50 – Gly – FITC

are quite similar, the labelled product still showing increments between neighbouring substates in geometrical progression and thus seeming to function essentially according to the 'barrel–stave' model. The amplitude histograms of Fig. 4, beside confirming a comparable distribution pattern, show that the most probable levels are in rough agreement with an N_{app} value of four–five, as obtained from the macroscopic conductance analysis. The main effect is obviously the lengthening of the duration of the open channels for the FITC analogue, as shown in Fig. 3 and analyzed for the various levels in Table 3. Fig. 5 gives examples of open lifetime distributions for the most probable subconductance level (substate number 2). This spectacular behaviour (ten–fifteen times slower) has already been observed between trichorzianins TB VII and TB III_c, which are 19 residue-long peptaibols, when the C-terminal Pheol is

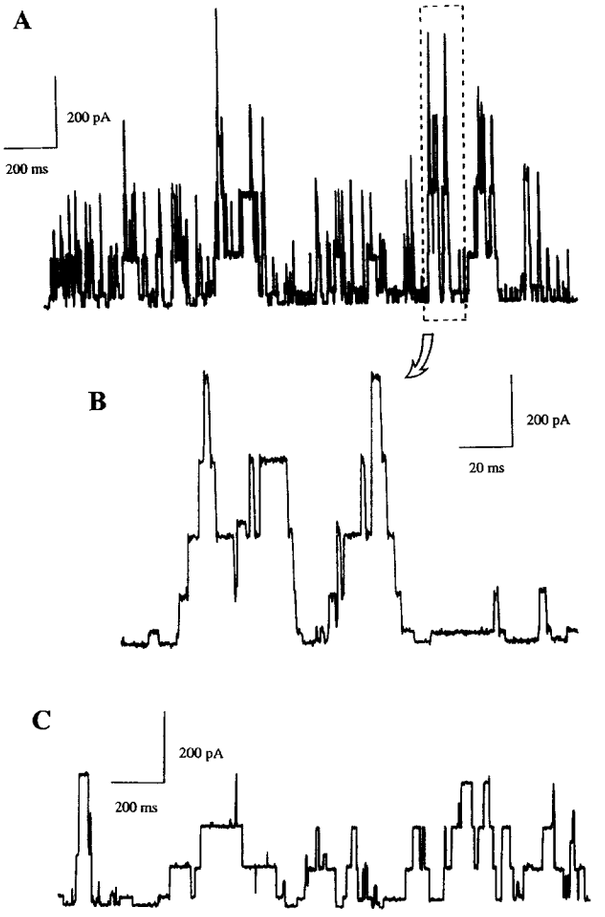

Fig. 3. Single-channel traces compared for Alm (A) and FITC–Gly–Alm (C) with the same current and time scales. Part B of the figure is an enlargement (the time base being ten times faster) of the delineated part of trace A. Lipids used for bilayer formation: POPC–DOPE (7:3, m/m), 1 M KCl both sides. Applied voltages: 140 mV (in A) and 80 mV (in C). The peptide concentrations were $6 \cdot 10^{-9}$ M in A and $4 \cdot 10^{-9}$ M in C. Room temperature as in Fig. 2.

replaced by Trpol, an indole group presenting a larger dipole moment [24]. As the FITC group possess more conjugated cycles than Trpol and, hence, of Pheol,

Table 3
Number of events and open lifetime values (in ms) for each subconductance state

Substates	1		2		3		4	
	Events	Lifetime	Events	Lifetime	Events	Lifetime	Events	Lifetime
Alamethicin Rf 50	1421	3.25	510	3.55	179	3.5	43	2.8
FITC–Gly–Alam	964	53.6	537	53.4	163	37	31	23

Sample rate and applied voltage are: 10 kHz and 140 mV for alamethicin Rf 50, and 3 kHz and 200 mV for FITC–Gly–Alam. Temperature, 25°C.

the Alm–Gly–FITC should present a stronger dipolar moment and thus would induce longer open lifetimes.

3.4. Lateral diffusion at rest and under applied voltage

The new fluorescent analogue of alamethicin, which retains the essential features of the native molecule, with the additional channel stabilization (an advantage in the proposed application), was then tested for its lateral diffusion within bilayers and under voltage with the FRAP method [17]. Preliminary FRAP experiments with PLBs equilibrated with aqueous concentrations of the labelled alamethicin in the range 10–100 nM (to match the conditions of Fig. 2 and yield macroscopic I–V curves for moderate voltage, below 100 mV) pointed to a significant contribution from the bulk fluorescence that precluded any meaningful estimates of D, the lateral diffusion coefficient, for the peptide associated with bilayers. To overcome this problem, the labelled peptide and lipids were pre-mixed in the desired ratio prior to forming the membrane. In addition, fluorescence recovery curves were recorded as soon as possible after PLB formation and a fast perfusion device was used in subsequent recordings, as the labelled peptide tends to diffuse out of the bilayer-as-

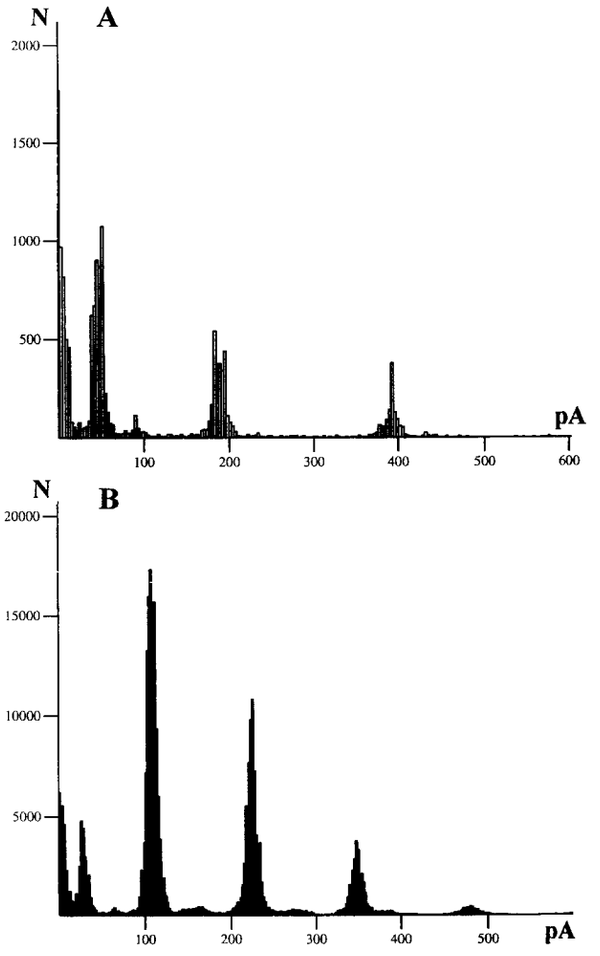

Fig. 4. Amplitude histograms (or current distribution) corresponding to long periods of activity including the traces. (A) is for alamethicin Rf 50 and (B) is for the fluorescein-labelled analogue.

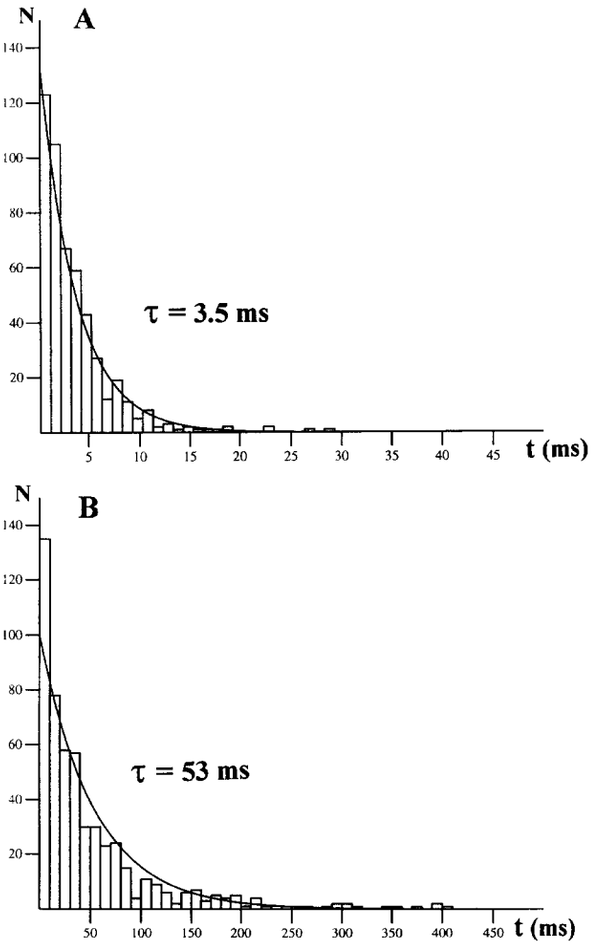

Fig. 5. Open channel lifetime histograms for substate 2, both for alamethicin Rf 50 (A) and FITC–Gly–Alam (B). Mean open times are given by τ, the time constant of the best-fitting exponential to the time distributions.

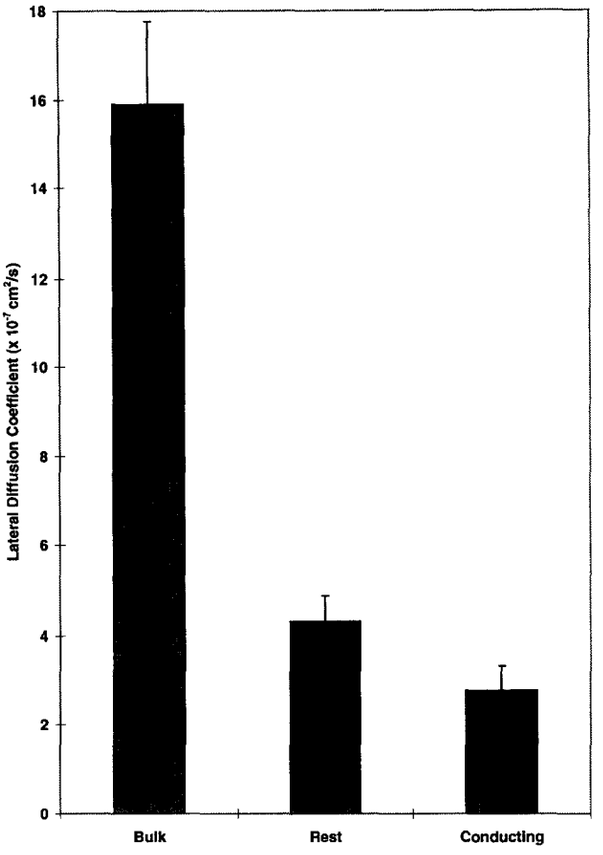

Fig. 6. Lateral diffusion of FITC–Gly–alamethicin in the bulk (1 M KCl, 5 mM HEPES, pH 7.4), in the membrane-associated state at rest (0 mV) and in the conducting state (for −30 to −50 mV, 10 nA).

sociated state to the surrounding bulk. Under these conditions, out of fifteen independent experiments, D at 0 mV averaged $4.3 \cdot 10^{-7}$ cm^2/s. This was much lower than the bulk diffusion of FITC–alamethicin, which was in the 10^{-7} M concentration range ($16 \cdot 10^{-7}$ cm^2/s), but it was faster than typical values for a lipid probe in the same system, i.e. $1.3 \cdot 10^{-7}$ cm^2/s [17]. Under applied voltages (typically −30 to −50 mV, of negative sign since the peptide was mostly on the *trans*-side) that are sufficient to induce a large current density of the order of 100 μA/cm^2 (I–V curves developing in the negative quadrant), the diffusion coefficient was reduced by a factor of nearly two (Fig. 6).

Previous studies with shorter alamethicin derivatives bearing the fluorescent dansyl group at the N-terminus showed the ability of these compounds to promote Ca^{2+} influx into liposomes and to uncouple oxidative phosphorylation in rat liver mitochondria [26]. Despite showing that labelling did preserve the essential functional properties of the parent molecule, a direct comparison with our study is not possible since no channel data was available in the above-mentioned work. Recent experiments with fluorescein-labelled pardaxin (a pore-forming neurotoxic peptide) demonstrated reversible surface aggregation and exchange of the peptide between liposomes [27]. Lateral diffusion determinations of pore-forming peptides have been reported previously for gramicidin [28] and, more recently, for a signal peptide of cytochrome c oxidase subunit IV [29]. In multibilayers, dansylated-gramicidin diffuses like a lipid molecule and, at high concentrations, restricts the lateral mobility of membrane components. The lateral diffusion of the signal peptide labelled with *N*-(7-nitrobenzoyl-2-oxa-1,3diazol-4-yl) (NBD) [29] was 1.5–1.6-fold faster than the phospholipid lateral diffusion in uncharged bilayers, in agreement with our own study. This suggests that alamethicin at rest is loosely associated on the membrane surface. The reduction of D observed under conditions promoting the open state of alamethicin supports either a further embedding of monomers into the bilayers or the building-up of conducting aggregates. However, D under these conditions is still faster than lipid diffusion. This is probably due to the fact that the FRAP technique detects an average diffusion of both monomers and conducting oligomers. Presumably, only a small proportion of membrane-associated alamethicin would actually be involved in pore-formation.

Acknowledgements

This work was supported by GdR 1153 CNRS "*Peptides et Protéines Amphipathiques*". The help of Dr. C. Fiol in fluorescence experiments is acknowledged. This work was initiated through a Franco–British Alliance program. Dr S. Ladha and A. Mackie were supported by CSG funding from the BBSRC. We thank Dr. E.J.A. Lea (University of East Anglia, Norwich, UK) for helpful discussions.

References

[1] G. Spach, H. Duclohier, G. Molle, J.-M. Valleton, Biochimie 71 (1989) 11–21.
[2] G.A. Wolley, B.A. Wallace, J. Membr. Biol. 129 (1992) 109–136.
[3] M.S.P. Sansom, Eur. Biophys. J. 22 (1993) 105–124.
[4] D.S. Cafiso, Annu. Rev. Biophys. Biomol. Struct. 23 (1994) 141–165.
[5] P. Mueller, D.O. Rudin, Nature 217 (1968) 713–719.
[6] G. Molle, J.-Y. Dugast, H. Duclohier, G. Spach, Biochim. Biophys. Acta 938 (1988) 310–314.
[7] H. Duclohier, G. Molle, J.-Y. Dugast, G. Spach, Biophys. J. 63 (1992) 868–873.
[8] G. Baumann, P. Mueller, J. Supramol. Struct. 2 (1974) 538–557.
[9] G. Boheim, J. Membr. Biol. 19 (1974) 277–303.
[10] J.D. Lear, Z.R. Wasserman, W.F. DeGrado, Science 240 (1988) 1177–1181.
[11] M. Montal, Annu. Rev. Biophys. Biomol. Struct. 24 (1995) 31–57.
[12] D. Marsh, Biochem. J. 315 (1996) 345–361.
[13] R.O. Fox, F.M. Richards, Nature 300 (1982) 277–303.
[14] W. Hanke, G. Boheim, Biochim. Biophys. Acta 596 (1980) 456–462.
[15] D.R. Laver, Biophys. J. 66 (1994) 355–359.
[16] L.K. Tam, in: S.H. White (ed.), Membrane Protein Structure, Oxford University Press, New York, 1994, pp. 283–313.
[17] S. Ladha, A.R. Mackie, L.J. Harvey, D.C. Clark, E.J.A. Lea, M. Brullemans, H. Duclohier, Biophys. J. 71 (1996) 1364–1373.
[18] J.R. Simon, D.L. Taylor, Methods Enzymol. 134 (1986) 487–507.
[19] G. Schwartz, H. Gerke, V. Rizzo, S. Stankowski, Biophys. J. 52 (1987) 685–692.
[20] G.A. Woolley, R.M. Epand, I.D. Kerr, M.S.P. Sansom, B.A. Wallace, Biochemistry 33 (1994) 6850–6858.
[21] M. Montal, P. Mueller, Proc. Natl. Acad. Sci. U.S.A. 69 (1972) 3561–3566.
[22] L.G.M. Gordon, D.A. Haydon, Phil. Trans. R. Soc. London B 270 (1975) 433–447.
[23] J.E. Hall, I. Vodyanoy, T.M. Balasubramanian, G.R. Marshall, Biophys. J. 45 (1984) 233–247.
[24] H. Duclohier, G. Molle, G. Spach, Biochim. Biophys. Acta 987 (1991) 133–136.
[25] D.-O.D. Mak, W.W. Webb, Biophys. J. 69 (1995) 2323–2336.
[26] M.K. Mathew, R. Nagaraj, P. Balaram, Biochim. Biophys. Acta 649 (1981) 336–342.
[27] D. Rapaport, R. Peled, S. Nir, Y. Shai, Biophys. J. 70 (1996) 2502–2512.
[28] D.W. Tank, E.S. Wu, P.R. Meers, W.W. Webb, Biophys. J. 40 (1982) 129–135.
[29] S. Frey, L.K. Tamm, Biochem. J. 272 (1990) 713–719.